



# Thermal, spectroscopic and dissolution studies of lovastatin solid dispersions with acetylsalicylic acid

Agata Górnica<sup>1</sup> · Maciej Gajda<sup>2</sup> · Janusz Pluta<sup>2</sup> · Hanna Czapor-Irzabek<sup>1</sup> ·  
Bożena Karolewicz<sup>2</sup>

Received: 10 August 2015 / Accepted: 16 January 2016 / Published online: 4 February 2016  
© The Author(s) 2016. This article is published with open access at [Springerlink.com](http://Springerlink.com)

**Abstract** Lovastatin (LOV) is widely used for the treatment of hypercholesterolemia. The poor water solubility of LOV leads to its poor gastrointestinal absorption and results in poor bioavailability. In this study, a preparation of solid dispersions with acetylsalicylic acid (ASA) was studied to improve the dissolution rate of LOV. Solid dispersions were prepared using various mass ratios of both components through the grinding method. Differential scanning calorimetry (DSC), Fourier transform infrared spectroscopy (FTIR) and X-ray powder diffraction (XRPD) were used to characterize prepared solid dispersions. Their dissolution behaviors were also compared. LOV and ASA formed a simple eutectic phase diagram as indicated by DSC. The results obtained from FTIR spectroscopy and XRPD showed no evidence of drug–drug interaction. The dissolution studies indicated that the *in vitro* dissolution rate of LOV released from solid dispersions containing 10, 20, 40 and 60 mass% LOV was improved compared with the drug alone.

**Keywords** Lovastatin · Acetylsalicylic acid · Phase diagram · Dissolution · Solid dispersion · DSC · FTIR · XRPD

## Introduction

Lovastatin, an active pharmaceutical ingredient (API) of drugs widely used for the treatment of hypercholesterolemia, is one of the competitive inhibitors of 3-hydroxy-3-methylglutaryl-coenzyme A (HMG-CoA) reductase [1]. This group of medicines is called statins, which, beyond their ability to lower serum cholesterol levels, is also known for their pleiotropic actions independent of lipid-lowering properties. These effects include improving endothelial dysfunction, decreasing vascular inflammation, inhibiting smooth-muscle proliferation and impacting on the coagulation system and fibrinolysis and immunomodulation [2–5]. Lovastatin is also a potent inhibitor of meningioma cell proliferation [6] and induces a specific apoptotic response in lung cancer cells within an achievable therapeutic range [7]. Lovastatin protects human endothelial cells from the genotoxic and cytotoxic effects of anticancer drugs [8].

Acetylsalicylic acid (ASA), known commonly as aspirin, prevents the aggregation of platelets and is recommended at low doses (75–325 mg daily) for patients to pharmacologically prevent cardiovascular disease besides an administration of cholesterol-lowering drugs [9, 10].

Combination therapy, in which two or more active pharmaceutical ingredients (APIs) are contained in a single dosage form, may cause an improvement in patient compliance and consequently increase the efficiency of therapy [11, 12]. For orally administered drugs, solubility is one of the most limiting parameters affecting their bioavailability [13]. Poor solubility of active ingredients causes great limitation in the absorption process of a drug. Lovastatin belongs to the II class of Biopharmaceutics Classification System (BCS) due to its high permeability and low water solubility ( $0.4 \mu\text{g mL}^{-1}$  [14]). Therefore, it can be assumed that improving its dissolution will improve its bioavailability. An effective and

✉ Agata Górnica  
[agata.gorniac@interia.pl](mailto:agata.gorniac@interia.pl); [agata.gorniac@umed.wroc.pl](mailto:agata.gorniac@umed.wroc.pl)

<sup>1</sup> Laboratory of Elemental Analysis and Structural Research, Wrocław Medical University, Borowska 211A, 50-556 Wrocław, Poland

<sup>2</sup> Department of Drug Form Technology, Wrocław Medical University, Borowska 211A, 50-556 Wrocław, Poland

convenient technique used to enhance the dissolution of poorly soluble drugs is the preparation of solid dispersion [15–17]. A lot of carriers have been employed in the preparation of lovastatin solid dispersions in order to improve the solubility of LOV, such as mannitol [18], Poloxamer F68 [19], polyethylene glycol 4000 and 6000, (PEG 4000, PEG 6000), polyvinylpyrrolidone K30 (PVP K30) [20, 21], sodium starch glycolate, croscarmellose sodium, crospovidone [22, 23], locust bean gum [24] and soluplus [25], but no reports exist on forming lovastatin solid dispersions with other APIs. Our previous research into binary mixtures of fenofibrate or simvastatin with ASA showed an appreciable increase in the API dissolution rate in relation to eutectic formations [26, 27]. In light of this, the aim of the present study was to characterize the solid state of the prepared LOV/ASA solid dispersions by DSC, FTIR and XRPD, as well as to assess the formation of LOV/ASA solid dispersions on the dissolution rate of both ingredients.

## Experimental

### Materials

Lovastatin (99 %) was obtained as a gift sample from Polpharma (Poland). ASA (99 %) was a commercially available product of Aldrich. Sodium lauryl sulfate (SLS) was purchased from Stanlab (Poland). Sodium hydrogen phosphate, potassium dihydrogen phosphate and phosphoric acid were purchased from Chempur (Poland). Acetonitrile (HPLC grade) was obtained from Fluka Biochemica (Germany).

### Preparation of solid dispersions

Finely powdered mixtures were prepared from accurately weighed quantities of each component using a Mettler Toledo AT 261 microbalance ( $\pm 0.01$  mg). Next, the mixtures were very thoroughly ground together for at least 10 min using an agate mortar and pestle. DSC studies confirmed that both components were stable after grinding. Nine solid dispersions of lovastatin and ASA were prepared. The mass ratios of the LOV/ASA dispersions were 10.0/90.0, 20.0/80.0, 30.0/70, 40.0/60.0, 50.0/50.0, 60.0/40.0, 70.0/30.0, 80.0/20.0 and 90.0/10.0 %, respectively. The pulverized mixtures were sieved using a 315- $\mu$ m sieve and then stored in a desiccator at room temperature until use.

### Drug content

The aspirin and lovastatin contents of the dispersions were found to be in the range of 98.19–102.50 % of the declared

**Table 1** Drugs content in prepared dispersions

Dispersion	Average content of LOV	Average content of ASA
10/90 LOV/ASA	98.19 $\pm$ 0.13	102.39 $\pm$ 0.17
20/80 LOV/ASA	99.39 $\pm$ 0.35	101.02 $\pm$ 0.25
30/70 LOV/ASA	100.41 $\pm$ 0.25	99.68 $\pm$ 0.20
40/60 LOV/ASA	101.90 $\pm$ 0.48	98.27 $\pm$ 0.26
50/50 LOV/ASA	101.96 $\pm$ 0.24	98.24 $\pm$ 0.34
60/40 LOV/ASA	102.50 $\pm$ 0.32	98.55 $\pm$ 0.17
70/30 LOV/ASA	101.79 $\pm$ 0.23	99.89 $\pm$ 0.10
80/20 LOV/ASA	102.42 $\pm$ 0.15	98.44 $\pm$ 0.19
90/10 LOV/ASA	102.10 $\pm$ 0.17	98.90 $\pm$ 0.35

Data are expressed as mean  $\pm$  SD ( $n = 3$ )

amounts. Table 1 lists the results from the investigations of drugs content in the dispersions.

### Differential scanning calorimetry (DSC)

The DSC curves of pure components and solid dispersion were obtained using a DSC 214 Polyma (Netzsch, Germany) heat flux type calorimeter. Measurement control and data analysis were performed with Proteus software (Netzsch, Germany). Samples for the DSC measurements were sealed in 40- $\mu$ l standard aluminum crucibles with a single hole punched in the lid. The total mass of a sample was between 4 and 6 mg. An empty crucible of the same type was used as a reference. The seven-point temperature calibration was performed using adamantane ( $-64.5$  °C), indium ( $156.6$  °C), tin ( $231.9$  °C), bismuth ( $271.4$  °C) and zinc ( $419.5$  °C) as a standard [28, 29]. The DSC cell was purged with a stream of high purity nitrogen (99.999 %) at a rate of  $25 \text{ cm}^3 \text{ min}^{-1}$ . DSC scans of all dispersions and pure components were run in triplicate at a heating rate of  $10 \text{ }^\circ\text{C min}^{-1}$  in the temperature range of 25–190 °C.

### X-Ray powder diffractometry (XRPD)

Powder X-ray diffraction patterns were collected on a D2 Phaser (Bruker, Germany) diffractometer, operating at 30 kV and 10 mA, with a  $\text{CuK}\alpha$  radiation and LYNXEYE detector. The powder samples were scanned over a  $2\theta$  range of  $5^\circ$ – $40^\circ$  with a step size of  $0.02^\circ$  and step time of 0.5 s.

### Fourier transform infrared spectroscopy (FTIR)

FTIR spectra were performed on Nicolet iS50 FTIR (Thermo Scientific, USA) spectrometer by using an attenuated total reflection (ATR) module. The spectra were scanned over a wavenumber range of  $4000$ – $400 \text{ cm}^{-1}$ .

### Intrinsic dissolution rate (IDR)

The intrinsic dissolution rate studies were carried out for pure LOV and all of the prepared solid dispersions of LOV/ASA. The dissolution studies were tested in water bath dissolution SR8-PLUS (Hanson, USA) fitted with a 7-channel peristaltic pump. The intrinsic dissolution rate was measured using the rotating disk method. LOV (100.0 mg) or an equivalent amount of solid dispersion disks were prepared by compressing powder in a Specac hydraulic press (Mettler Toledo, Switzerland) for 1 min under 1 t compression force, using a 8-mm punch. The die was mounted on the stirring drive mechanism and was rotated at 50 rpm. The dissolution test was conducted under sink conditions in 1000 mL of pH 7.0 phosphate buffer with 0.5 % SLS at  $37 \pm 0.5$  °C and rotational speeds of 50 rpm at  $37 \pm 0.5$  °C. Samples were withdrawn at appropriate time intervals. Quantitative determinations for LOV and ASA were performed with HPLC system (System GOLD 126, Beckman Coulter) with a UV-Vis detector. The analysis was carried out with the use of Zorbax SB-C8 (25 cm  $\times$  4.6 mm, 5  $\mu$ m, Agilent). HPLC analyses were performed by isocratic elution with a flow rate of 1.5 mL min<sup>-1</sup>. The mobile phase composition was acetonitrile–water (60:40) with 0.1 % phosphoric acid. Substances eluted from the column were identified by UV-Vis detector at 238 nm. External standards of LOV and ASA were used to obtain calibration curves. Linear calibration curves were obtained between 5 and 300  $\mu$ g mL<sup>-1</sup> for LOV and between 5 and 650  $\mu$ g mL<sup>-1</sup> for ASA.

### In vitro of LOV/ASA solid dispersions dissolving into hard gelatin capsule

Release studies were carried out in triplicate in USP Apparatus 2 (Basket type). Solid dispersions equivalent to 40 mg of the drug in gelatin capsules were added 500 mL of pH 7.0 phosphate buffer with 0.5 % SLS stirred at 75 rpm. Aliquots of 3 mL were withdrawn at specified time intervals and analyzed by HPLC at 238 nm.

## Results and discussion

### DSC study

The DSC curves of LOV, ASA and investigated dispersions obtained at a heating rate of 10 °C min<sup>-1</sup> in the temperature range from 25 to 190 °C are presented in Fig. 1. Pure LOV and ASA shows a characteristic endotherm peak ( $\Delta_{\text{fus}}H = 101.8$  and  $\Delta_{\text{fus}}H = 178.7$  J g<sup>-1</sup>, respectively) corresponding to melting points at 173.4 and 145.3 °C, respectively. The DSC curves of the various dispersions indicated that LOV and ASA formed a binary eutectic system. The phase diagram constructed on the basis of the DSC results is presented in Fig. 2. The DSC curves of investigated dispersions, presented in Fig. 1, demonstrated only two endothermic effects which have an outline characteristic for simple eutectic systems. The first sharp peak with a variable area appeared at the same temperature for all the dispersions, while the second peak

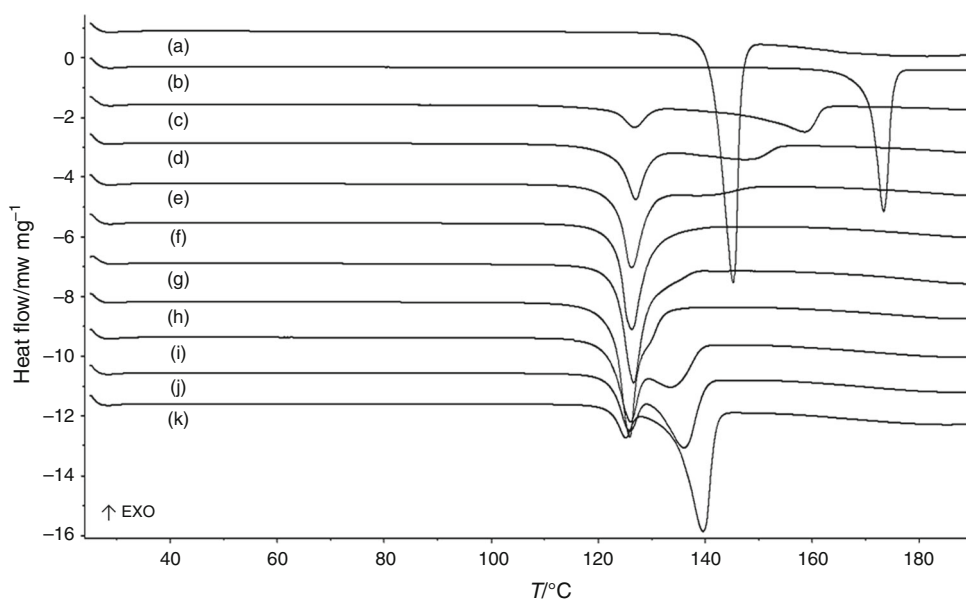


**Fig. 1** DSC curves of: ASA (a), LOV (b) and obtained LOV/ASA solid dispersions: 90/10 % w/w LOV/ASA (c), 80/20 % w/w LOV/ASA (d), 70/30 % w/w LOV/ASA (e), 60/40 % w/w LOV/ASA (f),

50/50 % w/w LOV/ASA (g), 40/60 % w/w LOV/ASA (h), 30/70 % w/w LOV/ASA (i), 20/80 % w/w LOV/ASA (j), 10/90 % w/w LOV/ASA (k)

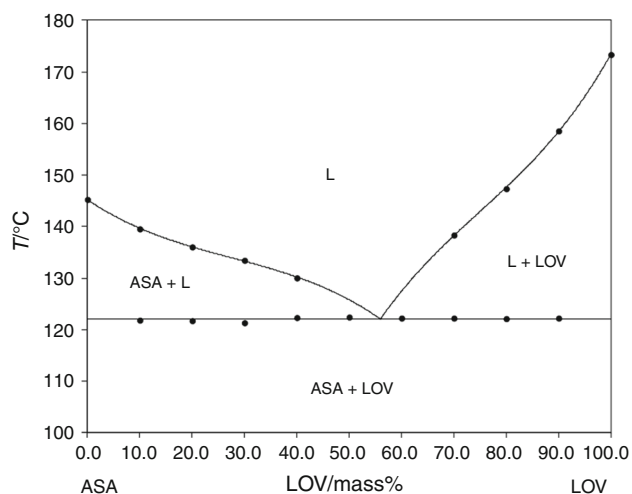


**Fig. 2** Phase equilibrium diagram of the LOV–ASA system

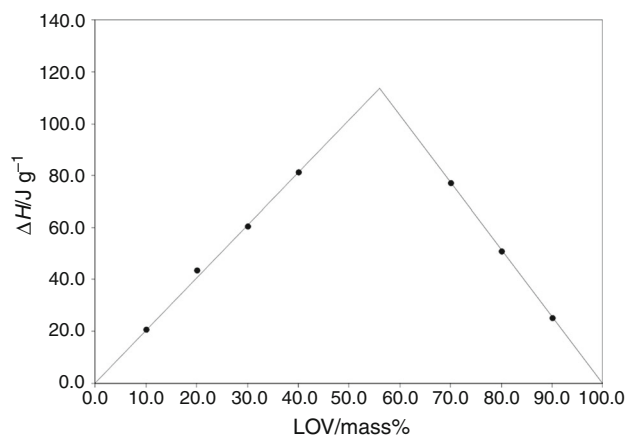


**Fig. 3** Tamman's triangle construction for the eutectic melting enthalpy  $\Delta H$  at 122.1 °C

was wider and appeared at different positions according to the mass ratios as shown in Fig. 1. The onset of the first peak near 122.1 °C does not vary with the mass ratio of LOV and indicates the temperature of the eutectic reaction: solid ASA + solid LOV = liquid (L). The thermal effect corresponding to the eutectic reaction was visible on DSC curves for most dispersions examined (Fig. 1). The values of the eutectic melting enthalpy  $\Delta H$  ( $\text{J g}^{-1}$ ) for a given dispersions, determined by integration of the eutectic peak area on DSC curves, are plotted in Fig. 3 versus mass ratio of LOV in order to construct Tamman's triangle [30]. The composition of the eutectic point, corresponding to the maximum value of enthalpy, has been found for 56.0 mass% of LOV, which is in agreement with the phase diagram (Fig. 2). The enthalpy of the eutectic transition goes to zero for compositions corresponding to pure components. This confirms that there is no mutual

miscibility in the solid state and no formation of terminal solid solutions at either side of the phase diagram.

### XRPD study

The diffraction spectra of LOV, ASA and dispersions with 80/20, 60/40, 40/60 and 20/80 LOV/ASA mass ratios, respectively, are presented in Fig. 4. The X-ray diffractograms of pure LOV and ASA shows the crystalline nature of drugs, as indicated by numerous distinctive peaks. Characteristic diffraction peaks occurred for LOV at approximately  $2\theta$  angles of 7.84°, 9.36°, 10.12°, 10.88°, 12.80°, 15.60°, 16.68°, 17.28°, 17.76°, 18.88°, 19.32°, 19.68°, 22.40°, 24.48°, 25.12°, 25.92°, 28.38°. The X-ray diffractogram of ASA shows characteristic distinctive sharp peaks at a diffraction  $2\theta$  angle of 7.76° and 15.60°, 26.92°. The diffractogram of the solid dispersion that contained 90 mass% of ASA exhibited the presence of distinctive peaks of crystalline second phase—LOV at  $2\theta$  of 9.36°, 17.76°, 18.88°, 19.68°, although their relative intensities were reduced. On the other hand, similar observations were noted on an X-ray diffractogram of 90 mass% LOV. It shows a slight amount of the crystalline ASA exhibited on the presence of distinctive peaks at  $2\theta$  of: 7.76° and 15.60°, 26.92°. These data confirmed that at room temperature the two components which formed the examined dispersions do not create solid solutions. Moreover, no other peaks than those that could be assigned to the LOV and ASA were detected in the diffraction patterns of dispersions, indicating an absence of chemical interaction in the solid state between the two entities.

### FTIR study

The FTIR spectra of pure drugs and their dispersions are presented in Fig. 5. The spectrum of pure LOV shows intense absorption bands at 3538  $\text{cm}^{-1}$  (alcohol O–H stretching), 3017  $\text{cm}^{-1}$  (olefinic C–H stretching), 2965  $\text{cm}^{-1}$  (methyl C–H asymmetric stretching), 2929  $\text{cm}^{-1}$  (methylene C–H asymmetric stretching), 2866  $\text{cm}^{-1}$  (methyl and methylene C–H asymmetric stretching), 1723, 1697  $\text{cm}^{-1}$  (lactone and ester carbonyl stretch), 1459  $\text{cm}^{-1}$  (methyl asymmetric bend), 1381  $\text{cm}^{-1}$  (methyl symmetric bend), 1260  $\text{cm}^{-1}$  (lactone C–O–C asymmetric bend), 1214  $\text{cm}^{-1}$  (ester C–O–C asymmetric bend), 1074  $\text{cm}^{-1}$  (lactone C–C symmetric bend), 1054  $\text{cm}^{-1}$  (ester C–O–C symmetric bend), 969  $\text{cm}^{-1}$  (alcohol C–OH stretch) and 870  $\text{cm}^{-1}$  (trisubstituted olefinic C–H). All major LOV peaks and absorption bands characteristic for ASA at 1604  $\text{cm}^{-1}$  (benzene ring stretching), at 1678 and 1749  $\text{cm}^{-1}$  (aliphatic carbonyls vibrations) and a broader band at 2500–3500  $\text{cm}^{-1}$  (carboxylic acid hydroxyl group stretching) appear in the spectra of examined dispersions at the same wavenumbers. The spectra show only a

**Fig. 4** XRPD patterns of: ASA (a), 10/90 % w/w LOV/ASA (b), 20/80 % w/w LOV/ASA (c), 40/60 % w/w LOV/ASA (d), 60/40 % w/w LOV/ASA (e), 80/20 % w/w LOV/ASA (f), 90/10 % w/w LOV/ASA (g), LOV (h)

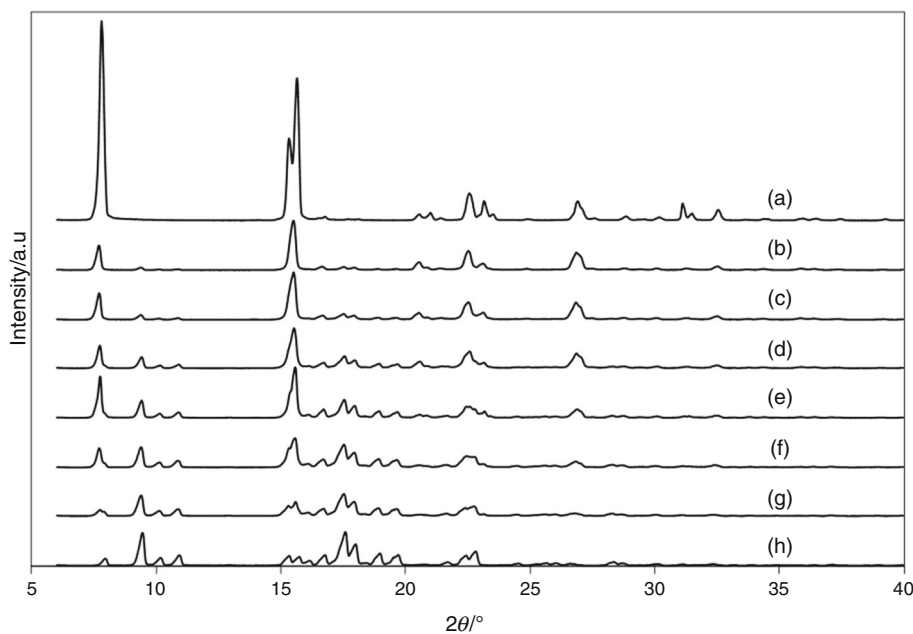
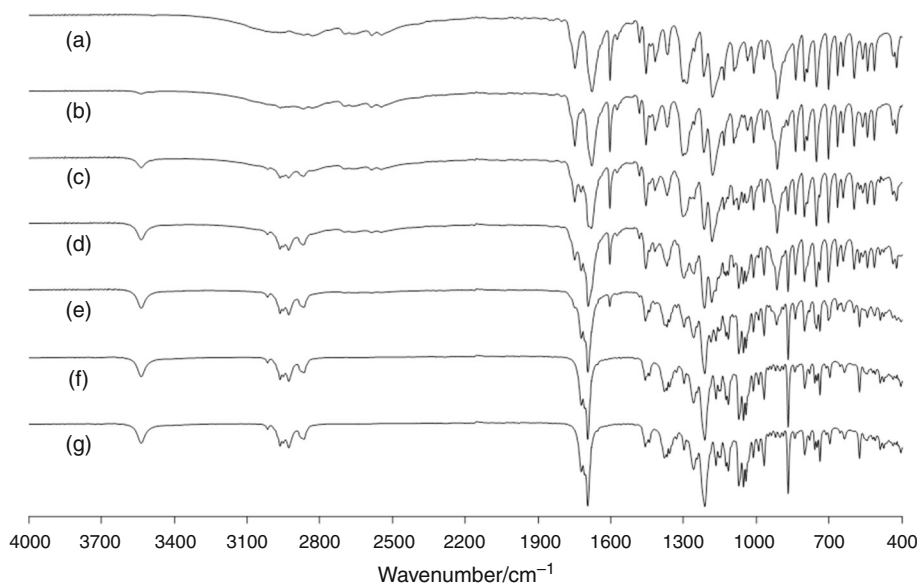


**Fig. 5** FTIR spectra of: ASA (a), 10/90 % w/w LOV/ASA (b), 30/70 % w/w LOV/ASA (c), 50/50 % w/w LOV/ASA (d), 70/30 % w/w LOV/ASA (e), 90/10 % w/w LOV/ASA (f), LOV (g)



reduction in the sharpness of peaks as compared to the spectra of pure components. The absence of a major shift in the observed peak positions indicates no interaction in the solid state between LOV and ASA.

### Dissolution studies

In Table 2, the IDR of the pure LOV and its solid dispersions with ASA in pH 7.0 phosphate buffer with 0.5 % SLS is summarized. Kaplan noted that compounds with an IDR below  $0.1 \text{ mg cm}^{-2} \text{ min}^{-1}$  usually exhibit a dissolution rate-limited absorption [31]. The IDR of pure LOV dissolved to pH 7.0

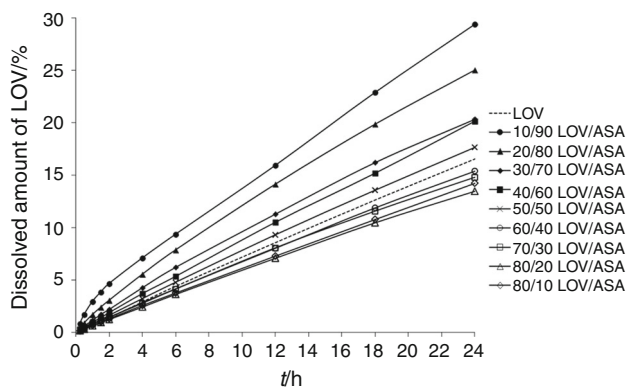
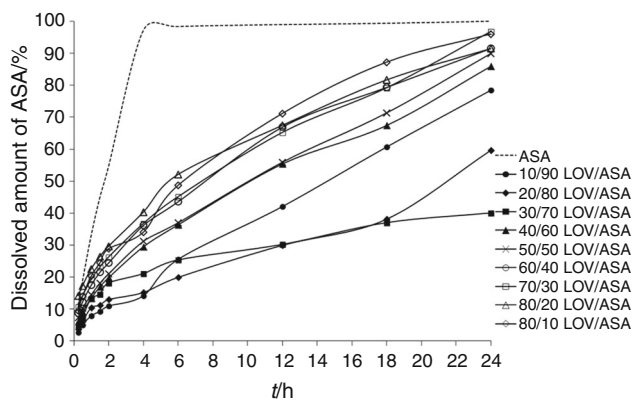
phosphate buffer with 0.5 % SLS was  $0.023 \text{ mg cm}^{-2} \text{ min}^{-1}$ , which makes it fall into this category. The intrinsic dissolution rate of LOV in solid dispersions containing the substance by mass percentage from 10, 20, 30, 40 and 50 % was higher. After 24 h of the test, almost 30 % of LOV was released from the solid dispersion containing 10 mass% of LOV, when at this time 16 % of pure LOV had been dissolved, as shown in Fig. 6. The dissolution rate of ASA from solid dispersions in conditions of constant surface area has not improved as shown in Fig. 7 and even has decreased. However, after 24 h of the test more than 50 % of ASA was released from most of the examined dispersions.



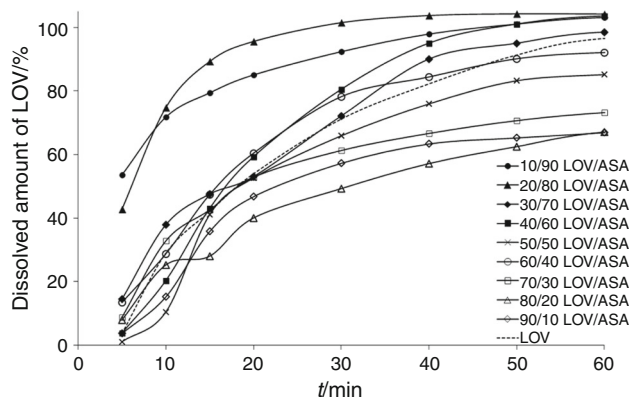
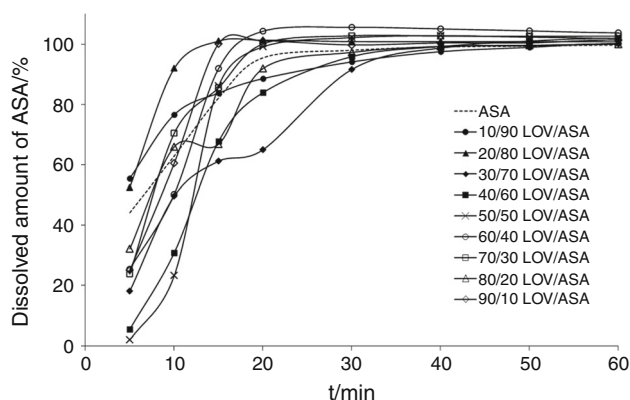
**Table 2** Intrinsic dissolution rate (IDR) of pure LOV and prepared dispersions (SDs), and corresponding ratios

Dispersion	IDR/mg cm <sup>-2</sup> min <sup>-1</sup>	r <sup>2</sup>	IDR ratio SDs/LOV
10/90 LOV/ASA	0.0400 ± 0.0002	0.9934	1.72
20/80 LOV/ASA	0.0350 ± 0.0001	0.9952	1.52
30/70 LOV/ASA	0.0290 ± 0.0002	0.9964	1.25
40/60 LOV/ASA	0.0280 ± 0.0002	0.9995	1.21
50/50 LOV/ASA	0.0250 ± 0.0007	0.9993	1.07
60/40 LOV/ASA	0.0220 ± 0.0001	0.9994	0.93
70/30 LOV/ASA	0.0210 ± 0.0010	0.9986	0.90
80/20 LOV/ASA	0.0190 ± 0.0004	0.9993	0.82
90/10 LOV/ASA	0.0200 ± 0.0007	0.9997	0.86
LOV	0.0230 ± 0.0004	0.9995	–

Data are expressed as mean ± SD (*n* = 3)

**Fig. 6** Dissolved amount of LOV from LOV/ASA solid dispersions within 24 h of dissolution process compared with pure LOV**Fig. 7** Dissolved amount of ASA from LOV/ASA solid dispersions within 24 h of dissolution process compared with pure ASA

In vitro results of LOV and ASA dissolving into a hard gelatin capsule in pH 7.0 phosphate buffer with 0.5 % SLS over a period of 60 min are shown in Figs. 8 and 9, respectively. The dissolution rate of LOV from solid dispersions

**Fig. 8** Dissolution profiles of LOV from LOV/ASA solid dispersions in the hard gelatin capsules**Fig. 9** Dissolution profiles of ASA from LOV/ASA solid dispersions in the hard gelatin capsules

10/90 LOV/ASA, 20/80 LOV/ASA, 40/60 LOV/ASA and 60/40 LOV/ASA were higher (85.1, 95.6, 59.3 and 60.4 %, respectively) than that of pure LOV (53.9 %) within 20 min. The dissolution rate tests carried out by both methods show that the improvement in the dissolution rate of LOV was observed for solid dispersions with the LOV mass content near and below the eutectic composition. The most likely reason for this was that the progress of dissolution was determined by the high content of ASA, which improves the dissolution of LOV and causes it to move more quickly to the solution. The results obtained allow the development of the most advantageous combinations in an oral dosage form with modified physical properties containing both ingredients in the range of desired therapeutic concentrations, i.e., LOV in the range of 10–40 mg and 75–100 mg of ASA.

## Conclusions

In this study, the grinding method was successfully applied to obtain solid dispersions of two BCS class II drugs, lovastatin and ASA. The DSC investigation has revealed

that LOV and ASA form a simple eutectic phase diagram. FTIR spectroscopy and XRPD studies of obtained dispersions showed no interaction between the components in the solid state and confirmed the absence of terminal solid solutions. The obtained in vitro dissolution results indicate that the formation of lovastatin solid dispersions with ASA could be a promising approach to improve its release from oral dosage form, and hence may affect its bioavailability. The improvement of the LOV dissolution rate does not depend directly on a eutectic composition, as in the case of simvastatin [27], that has water solubility one order of magnitude better ( $30 \mu\text{g mL}^{-1}$  [32]) than LOV, but the formation of eutectic in the LOV–ASA system naturally promotes the effective wetting of the reduced drug particles released from eutectic composition. The results of our investigation show that lovastatin dissolution rate can be improved by the formation of solid dispersions with ASA without chemical interaction between the drugs. This method could develop new oral pharmaceutical preparations with an expanded therapeutic spectrum for the treatment of cardiovascular diseases.

**Open Access** This article is distributed under the terms of the Creative Commons Attribution 4.0 International License (<http://creativecommons.org/licenses/by/4.0/>), which permits unrestricted use, distribution, and reproduction in any medium, provided you give appropriate credit to the original author(s) and the source, provide a link to the Creative Commons license, and indicate if changes were made.

## References

1. Tobert JA. Lovastatin and beyond: the history of the HMG-CoA reductase inhibitors. *Nat Rev Drug Discov.* 2003;2:517–26.
2. Pella D, Rybar R, Mechirova V. Pleiotropic effects of statins. *Acta Cardiol Sin.* 2005;21:190–8.
3. Wang Ch-Y, Liu P-Y, Liao JK. Pleiotropic effects of statin therapy: molecular mechanisms and clinical results. *Trends Mol Med.* 2008;14:37–44.
4. Reilly SD, Litovsky SH, Steinkampf MP, Caulfield JB. Statins improve human coronary atherosclerotic plaque morphology. *Tex Heart Inst J.* 2008;35:99–103.
5. Pasterkamp G, van Lammere GW. Pleiotropic effects of statins in atherosclerotic disease. *Expert Rev Cardiovasc Ther.* 2010;8:1235–7.
6. Johnson MD, Woodard A, Okediji EJ, Toms SA, Allen GS. Lovastatin is a potent inhibitor of meningioma cell proliferation: evidence for inhibition of a mitogen associated protein kinase. *J Neurooncol.* 2002;56:133–42.
7. Maksimova E, Yie T-A, Rom WN. In vitro mechanisms of lovastatin on lung cancer cell lines as a potential chemopreventive agent. *Lung.* 2008;186:45–54.
8. Damrot J, Nübel T, Epe B, Roos WP, Kaina B, Fritz G. Lovastatin protects human endothelial cells from the genotoxic and cytotoxic effects of the anticancer drugs doxorubicin and etoposide. *Br J Pharmacol.* 2006;149:988–97.
9. Eidelman RS, Hebert PR, Weisman SM, Hennekens ChH. An update on aspirin in the primary prevention of cardiovascular disease. *Arch Intern Med.* 2003;163:2006–10.
10. Chapman MJ. From pathophysiology to targeted therapy for atherothrombosis: a role for the combination of statin and aspirin in secondary prevention. *Pharmacol Ther.* 2007;11:184–96.
11. Wan X, Ma P, Zhang X. A promising choice in hypertension treatment: fixed-dose combinations. *Asian J Pharm Sci.* 2014;9:1–7.
12. Jin J, Sklar GE, Oh VMS, Li SC. Factors affecting therapeutic compliance: a review from the patient's perspective. *Ther Clin Risk Manag.* 2008;4:269–86.
13. Amidon GL, Lennernäs H, Shah VP, Crison JR. A theoretical basis for a biopharmaceutical drug classification: the correlation of in vitro drug product dissolution and in vivo bioavailability. *Pharm Res.* 1995;12:413–20.
14. Gerald SB, Dean KE, Micheal JK. Lovastatin. In: Brittain HG, editor. *Analytical profiles of drug substances and excipients*, vol. 21. New York: Academic Press; 1992. p. 277–315.
15. Moore MD, Wildfong PLD. Aqueous solubility enhancement through engineering of binary solid composites: pharmaceutical applications. *J Pharm Innov.* 2009;4:36–49.
16. Alam MA, Ali R, Al-Jenoobi FI, Al-Mohizea AM. Solid dispersions: a strategy for poorly aqueous soluble drugs and technology updates. *Expert Opin Drug Deliv.* 2012;9:1419–40.
17. Veronez IP, Daniel JSP, Júnior CEC, Garcia JS, Marcello G, Trevisan MG. Development, characterization, and stability studies of ethinyl estradiol solid dispersion. *J Therm Anal Calorim.* 2015;120:573–81.
18. Verma U, Naik JB, Mokale VJ. Preparation of freeze-dried solid dispersion powder using mannitol to enhance solubility of lovastatin and development of sustained release tablet dosage form. *AJPSN.* 2014;1:11–26.
19. Katare MK, Kohli S, Jain AP. Evaluation of dissolution enhancement of lovastatin by solid dispersion technique. *Int J Pharm Life Sci.* 2011;2:894–8.
20. Patel RP, Patel MM. Physicochemical characterization and dissolution study of solid dispersions of lovastatin with polyethylene glycol 4000 and polyvinylpyrrolidone K30. *Pharm Dev Technol.* 2007;12:21–33.
21. Neduri K, Bonthai VK, Vemula SK. Different techniques to enhance the dissolution rate of lovastatin: formulation and evaluation. *Asian J Pharm Clin Res.* 2013;6:56–60.
22. Vidyadhara S, Ramana Reddy GV, Ramu A, Chandana P. Formulation and evaluation of lovastatin fast dissolving tablets using newer super disintegrants. *J Pharm Res.* 2011;4:1762–5.
23. Shaikh K, Patwekar S, Payghan S, D'Souza J. Dissolution and stability enhancement of poorly water soluble drug—lovastatin by preparing solid dispersions. *Asian J Biomed Pharm Sci.* 2011;1:24–31.
24. Patel M, Tekade A, Gattani S, Surana S. Solubility enhancement of lovastatin by modified locust bean gum using solid dispersion techniques. *AAPS Pharm Sci Tech.* 2008;9:1262–9.
25. Raja Rajeswari K, Abbulu K, Sudhakar M, Vishwanadhami M, Tejaswini MS. Studies on dissolution enhancement of lovastatin using soluplus by solid dispersion technique. *Int J Pharm Pharm Sci.* 2012;4:124–8.
26. Górnaiak A, Wojakowska A, Karolewicz B, Pluta J. Phase diagram and dissolution studies of the fenofibrate–acetylsalicylic acid system. *J Therm Anal Calorim.* 2011;104:1195–200.
27. Górnaiak A, Karolewicz B, Żurawska-Plaksej E, Pluta J. Thermal, spectroscopic, and dissolution studies of the simvastatin–acetylsalicylic acid mixtures. *J Therm Anal Calorim.* 2013;111:2125–32.
28. van Ekeren PJ, van Genderen ACG, van den Berg GJK. Redetermination of the thermodynamic properties of the solid–solid transition of adamantane by adiabatic calorimetry to investigate the suitability as a reference material for low-temperature DSC-calibration. *Thermochim Acta.* 2006;446:33–5.

29. Della Gatta G, Richardson MJ, Sarge SM, Stolen S. Standards, calibration and guidelines in microcalorimetry. Part 2. Calibration standards for differential scanning calorimetry (IUPAC technical report). *Pure Appl Chem.* 2006;78:1455–76.
30. Rycerz L. Practical remarks concerning phase diagrams determination on the basis of differential scanning calorimetry measurements. *J Therm Anal Calorim.* 2013;113:231–8.
31. Kaplan SA. Biopharmaceutical considerations in drug formation design and evaluation. *Drug Metab Rev.* 1972;1:15–34.
32. Ellison DK, Moore WD, Petts CR. Simvastatin. In: Brittain HG, editor. *Analytical profiles of drug substances and excipients.* San Diego: Academic Press; 1993. p. 359–88.